SLEEPJ, 2021, 1–11

doi: 10.1093/sleep/zsab046
Advance Access Publication Date: 24 February 2021
Original Article

ORIGINAL ARTICLE

Leptin receptor expression in the dorsomedial hypothalamus stimulates breathing during NREM sleep in *db/db* mice

Huy Pho[1], Slava Berger[1], Carla Freire[1,*], Lenise J. Kim[1], Mi-Kyung Shin[1], Stone R. Streeter[1], Nishitha Hosamane[1], Meaghan E. Cabassa[1], Frederick Anokye-Danso[2], Olga Dergacheva[3,*], Mateus R. Amorim[1], Thomaz Fleury-Curado[1], Jonathan C. Jun[1,*], Alan R. Schwartz[1,4], Rexford S. Ahima[2], David Mendelowitz[3], and Vsevolod Y. Polotsky[1,*]

[1]Division of Pulmonary and Critical Care Medicine, Department of Medicine, Johns Hopkins University School of Medicine, Baltimore, MD, USA, [2]Division of Endocrinology, Diabetes, and Metabolism, Department of Medicine, Johns Hopkins University School of Medicine, Baltimore, MD, USA, [3]Department of Pharmacology and Physiology, George Washington University, Washington, DC, USA and [4]Department of Otorhinolaryngology, University of Pennsylvania Perelman School of Medicine, Philadelphia, PA, USA

*Corresponding author. Vsevolod (Seva) Y. Polotsky, Division of Pulmonary and Critical Care Medicine, Department of Medicine, The Johns Hopkins University School of Medicine, 5501 Hopkins Bayview Circle, Johns Hopkins Asthma and Allergy Center, Rm 4B65, Baltimore, MD 21224. Email: vpolots1@jhmi.edu.

Abstract

Study Objectives: Obesity leads to obstructive sleep apnea (OSA), which is recurrent upper airway obstruction during sleep, and obesity hypoventilation syndrome (OHS), hypoventilation during sleep resulting in daytime hypercapnia. Impaired leptin signaling in the brain was implicated in both conditions, but mechanisms are unknown. We have previously shown that leptin stimulates breathing and treats OSA and OHS in leptin-deficient *ob/ob* mice and leptin-resistant diet-induced obese mice and that leptin's respiratory effects may occur in the dorsomedial hypothalamus (DMH). We hypothesized that leptin receptor $LepR^b$-deficient *db/db* mice have obesity hypoventilation and that restoration of leptin signaling in the DMH will increase ventilation during sleep in these animals.

Methods: We measured arterial blood gas in unanesthetized awake *db/db* mice. We subsequently infected these animals with *Ad-LepR*^{b} or control *Ad-mCherry* virus into the DMH and measured ventilation during sleep as well as CO_2 production after intracerebroventricular (ICV) infusions of phosphate-buffered saline or leptin.

Results: Awake *db/db* mice had elevated CO_2 levels in the arterial blood. *Ad-LepR*^{b} infection resulted in *LepR*^{b} expression in the DMH neurons in a similar fashion to wildtype mice. In *LepR*^{b}-DMH *db/db* mice, ICV leptin shortened REM sleep and increased inspiratory flow, tidal volume, and minute ventilation during NREM sleep without any effect on the quality of NREM sleep or CO_2 production. Leptin had no effect on upper airway obstruction in these animals.

Conclusion: Leptin stimulates breathing and treats obesity hypoventilation acting on $LepR^b$-positive neurons in the DMH.

Statement of Significance

There is no pharmacotherapy for sleep-disordered breathing. Leptin has been implicated in the pathogenesis of sleep-disordered breathing, but a critical gap in understanding of mechanisms of leptin's action hindered its therapeutic use. This paper provided first evidence that leptin stimulates ventilation during sleep by acting on leptin receptor positive neurons in the dorsomedial hypothalamus. Furthermore, we demonstrated that these neurons uniformly express melanocortin 4 receptors, a part of an important metabolic pathway in obesity. Further investigation of leptin and melanocortin 4 signaling in the dorsomedial hypothalamus and projections of leptin receptor positive neurons at this location to respiratory control centers in the brainstem may lead to new therapies for sleep disordered breathing.

Key words: obstructive sleep apnea; leptin; dorsomedial hypothalamus; obesity

Submitted: 5 November, 2020; **Revised:** 6 February, 2021
© The Author(s) 2021. Published by Oxford University Press on behalf of Sleep Research Society. All rights reserved. For permissions, please e-mail: journals.permissions@oup.com

Introduction

Obesity is a highly prevalent condition observed in 34.9% of U.S. adults [1]. Obesity causes sleep-disordered breathing (SDB), which can be manifested by obstructive sleep apnea (OSA) and obesity hypoventilation syndrome (OHS). OSA is the most prevalent SDB, affecting 50% of obese patients [2–5]. OSA is characterized as recurrent obstructions of the upper airway during sleep, leading to intermittent hypoxia, sleep fragmentation, and intrathoracic pressure swings [6, 7]. OHS is defined by sleep-related decreases in ventilatory drive, leading to daytime hypercapnia and hypoventilation during sleep in obese individuals and it has been reported in 10%–20% of obese patients with OSA [8]. Continuous positive airway pressure (CPAP) is an efficacious treatment for both OSA [9, 10] and OHS [11]. Nevertheless, poor adherence to CPAP [12] limits its therapeutic use and emphasizes the unmet need for pharmacotherapy development. Pharmacological development in SDB has been hindered by the lack of rodent models of OSA.

We developed and validated novel plethysmographic methods for monitoring high-fidelity airflow and respiratory effort signals *continuously* during sleep in mice [13]. Upper airway obstruction was defined by the presence of inspiratory airflow limitation characterized by an early inspiratory plateau in airflow at a maximum level ($V_I$max) while effort continued to increase [13–16]. Moreover, we have demonstrated that obesity plays a major role in the pathogenesis of inspiratory flow limitation and OSA in mice and human alike [17–23].

Leptin is an adipocyte-produced hormone that regulates food intake and metabolic rate [24–26]. Leptin also plays an important role in the control of breathing [27] and upper airway patency [20, 28–30] during sleep [18, 19]. Leptin-deficient *ob/ob* mice develop SDB, characterized by (1) hypoventilation during sleep and the elevated partial pressure of carbon dioxide in the arterial blood ($PaCO_2$) [27]; (2) inspiratory flow limitation and recurrent hypopneas, similar to human OSA, which were reversed by leptin infusion [18, 19]. However, hyperleptinemia is a common feature of human obesity [29, 30] and obese humans are resistant to metabolic effects of leptin. Moreover, OSA and obesity hypoventilation are also associated with leptin resistance [28, 31, 32] and non-invasive ventilation decreases both CO_2 levels and leptin levels, independent of obesity [33]. The blood–brain barrier is one of the key sites of leptin resistance [34, 35]. Leptin delivery beyond the blood–brain barrier effectively reverses OSA and hypoventilation in both leptin-deficient and leptin-resistant mice [19, 20, 36]. Leptin signals *via* the long isoform of leptin receptor, $LepR^b$ [37–40], which is ubiquitous in the hypothalamus and many areas of medulla [41]. However, localization of respiratory effects of leptin and identity of leptin-responsive respiratory neurons remain unknown.

We have previously injected leptin into the lateral and fourth cerebral ventricles of *ob/ob* mice and found that leptin's effects on upper airway patency likely occur in the forebrain rather than in the medulla. We also found that hypoglossal motoneurons are synaptically connected to the dorsomedial hypothalamus (DMH), which abundantly expresses $LepR^b$ [19]. Notably, the DMH abundantly expresses another important metabolic receptor, melanocortin 4 receptor (MC4), which may mediate leptin's effect [42]. MC4 deficiency leads to severe obesity [43, 44] and has been associated with SDB [45]. We hypothesized that leptin's effect on SDB may occur via $LepR^b$ signaling in the DMH. In order to examine this hypothesis, we expressed $LepR^b$ exclusively in the DMH of obese $LepR^b$-deficient *db/db* mice and performed sleep studies after transgene expression at baseline and after intracerebroventricular (ICV) leptin infusion.

Methods

Animals

In total, 46 male homozygous B6.BKS(D)-Lep^{db}/J (*db/db*) leptin receptor deficient mice from Jackson Laboratory (Bar Harbor, ME, Stock #000697) were used for this study. $LepR^b$-*GFP* mice (n = 4) generated by breeding $LepR^b$-*Cre* [B6.129(Cg)-*Leprtm2(cre)*Rck/J, Stock #008320] and green fluorescent protein (GFP) floxed mice [B6.129-Gt(ROSA)26Sortm2Sho/J, Stock #004077] from the Jackson Laboratory were used for histology only. Water and food were available *ad libitum*. Mice were housed at a 12 h-light/dark cycle (7 am to 7 pm lights on), and temperature of 26°C. Food consumption and body weight were monitored daily throughout the sleep study protocol. All protocols were approved by the Johns Hopkins University Animal Care and Use Committee (ACUC) and all animal experiments were conducted in accordance with ACUC guidelines.

Arterial blood gas

Seven *db/db* mice had an arterial catheter implanted in the left femoral artery under 1%–2% anesthesia as previously described [14, 46]. In brief, a small incision was made to expose the femoral artery and an arterial catheter was placed 5–8 mm deep into the femoral artery. The catheter was glued in place and fed subcutaneously to be dorsally attached to a single channel fluid swivel (model 375/25, Instatech Laboratories, Plymouth Meeting, PA, USA), which slowly perfused a heparin saline solution (1,000 U heparin/L saline) *via* an infusion pump (0.5 mL/day). Mice recovered for 48–72 h. Arterial blood gas was analyzed in awake unrestrained unanesthetized mice by removing 150 µL of arterial blood, which was tested in a blood gas analyzer (Radiometer ABL 800 Flex, Diamond Diagnostics, Holliston, MA, USA).

Sleep studies

A two-arm crossover study design was used (Figure 1). Mice were randomized to receive stereotactic injections of *Ad-*$LepR^b$ or *Ad-mCherry*. After the 9-day gene expression period, each mouse was recorded with treatment of either ICV vehicle (phosphate

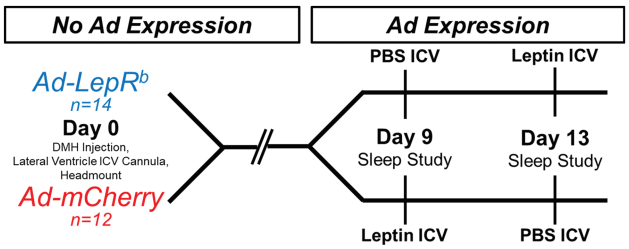

Figure 1. Experimental study design. $LepR^b$-deficient *db/db* mice were randomly transfected with *Ad-*$LepR^b$ or *Ad-mCherry* in the dorsomedial hypothalamus (DMH). Mice received intracerebroventricular (ICV) infusions of either PBS or leptin in a cross-over design and underwent polysomnography at days 9 and 13 after injection. $LepR^b$: long isoform of leptin receptor.

buffered saline, PBS) or ICV leptin. Polysomnography was performed in 26 mice, aged 15 weeks, at two time points with a 72-h washout period between studies.

Mice were anesthetized with isoflurane 1%–2% and placed in the stereotaxic system (Model 963 with 923-B Head Holder, David Kopf Instruments, Tunjunga, CA) and ~125 μL bilateral viral injections of either *Ad-LepR*^{b} (ADV-263380, Vector Biosystems, 2–5 × 10^{10} PFU/mL) or *Ad-mCherry* (Cat No: 1767, Vector Biolabs, 1 × 10^{10} PFU/mL) were performed using –1.88 mm caudal, ±0.40 mm lateral, –5.00 mm ventral as DMH coordinates from the bregma. To allow ICV administration of leptin or vehicle, a cannula (PlasticsOne, Roanoke, VA) was implanted in the right lateral ventricle at –0.60 mm caudal, –1.20 mm lateral, –3.00 mm ventral from the bregma. Headmount procedure was performed immediately following viral transfection and ICV cannula placement. Custom 6-pin headmounts (8231-SM-C, Pinnacle Technology, Lawrence, KS) were implanted for electroencephalogram (EEG) and electromyogram (EMG) recordings. Briefly, three holes were bored through the skull in the left and right frontal regions and left parietal region to allow implantation of 0.10″ silver electrodes with wire leads (no. 8403, Pinnacle Technology). The EEG leads from the custom headmount were twisted together with the three silver electrodes and coated with silver conductive epoxy (no. 8331, MG Chemicals) to provide unipolar conductive EEG electrodes. EMG leads were tunneled subcutaneously and placed over the nuchal muscle posterior to the skull. Dental acrylic (Lang Dental, Wheeling, IL) was used to secure the headmount and cannula in place.

For polysomnography we used a modified whole body plethysmography (WBP) chamber system to measure tidal airflow and sleep–wake state continuously, generating high-fidelity tidal volume and airflow signals, as previously described [13]. In brief, following ICV treatment of PBS (pH 7.4, 2 μL) or leptin (10 μg in 2 μL of PBS), mice were placed in the WBP chamber to be recorded from 10:00 am to 4:00 pm. Mice were weighted prior to sleep recording. Mouse rectal temperature was measured and averaged between beginning and end of sleep study. Mice were acclimated to the chamber prior to recording for at least 3 days, 1 h/day. During full polysomnographic recordings, the chamber was humidified to ~90% relative humidity and ~29°C while a slow leak allowed atmospheric pressure equilibrium. The WBP's reference chamber filtered out ambient noise from the pressure signal acquired by a transducer (Emka Technologies). Positive and negative pressure sources were utilized in series with mass flow controllers (Alicat Scientific) and high-resistance elements to generate a continuous bias airflow through the animal chamber while maintaining a sufficiently high time constant. Tidal airflow was calculated from the plethysmography chamber pressure signal using the Drorbaugh and Fenn equation [47], which required the measurements of mouse rectal temperature, chamber temperature, room temperature, relative humidity, and chamber gas constant, calculated by utilizing a known volume injection and the resultant chamber pressure deflection. The tidal volume signal was differentiated electronically to generate an airflow signal.

All signals were digitized at 1,000 Hz (sampling frequency per channel) and recorded in LabChart 7 Pro (Version 7.2, ADInstruments, Dunedin, NZ). Sleep–wake state was scored visually in 5 s epochs based off standard criteria of EEG and EMG frequency content and amplitude, as previously described [14, 18, 19]. Wakefulness was characterized by low-amplitude, high-frequency (~10–20 Hz) EEG waves and high levels of EMG activity compared with the sleep states. NREM sleep was characterized by high-amplitude, low frequency (~2–5 Hz) EEG waves with EMG activity considerably less than during wakefulness. REM sleep was characterized by low-amplitude, mixed frequency (~5–10 Hz) EEG waves with EMG amplitude either below or equal to that during NREM sleep. Respiratory signals were analyzed from all REM sleep periods and from periods of NREM sleep sampled periodically at 20-s stretches every half an hour throughout the total recording time. Custom software was used to demarcate the start and end of inspiration and expiration for subsequent calculations of timing and amplitude parameters for each respiratory cycle.

We utilized each breath's respiratory characteristic to describe maximal inspiratory airflow ($V_I$max) and components of minute ventilation (V_E). We developed an algorithm using the airflow and respiratory effort signals to determine if a breath was classified as inspiratory airflow limited, defined by an early inspiratory plateau in airflow while effort continued to increase. The software provided peak flow values during the first half ($V_I$max1), midpoint (V_I50), and second half ($V_I$max2) of inspiration. Breaths resembling sniffs were initially defined as non-flow limited by their short duration, having an inspiration time with a z-score lower than 1.75. Breaths having sufficient inspiration time were then classified as inspiratory flow limited if a mid-inspiratory flow plateau was present [14, 18, 19].

Metabolic measurements

Metabolic studies were performed in a separate subset of mice (n = 4 in the *Ad-LepR*^{b} group and n = 5 in the *Ad-mCherry* group) according to the design described for the sleep studies starting nine days after viral injection and cannula implantation (Figure 1), except that the headmount was not installed and the washout period was 1 week between studies. Mice were placed in individual Comprehensive Laboratory Animal Monitoring System (CLAMS) units (Oxymax series; Columbus Instruments, Columbus, OH) for a 24-h acclimation period followed by 48 h of continuous recordings. The 48-h recordings started at 10:00 am with four brief interruptions (daily at 10:00 am and 6:00 pm) for ICV injections. Each treatment infusion was 2 μL of PBS or leptin (10 μg/2 μL, R&D Systems, Minneapolis, MN). Data collected 30 min prior and 30 min after the ICV injections were excluded from the analysis. The CLAMS units were sealed and equipped with O_2 electrochemical sensors, CO_2 infrared sensors and infrared beam movement sensors. Consumed O_2 (VO_2) and produced CO_2 (VCO_2) were collected every 11 min and measurements were utilized to calculate the respiratory exchange ratio (RER). Motor activity was quantified by the number of infrared beam interruptions. Total horizontal and vertical beam breaks were summed and presented as motor activity. Metabolic cages were kept in a 12 h light/dark cycle (7 am to 7 pm lights on) with food and water *ad libitum* and a consistent environmental temperature of 24°C.

Immunofluorescence

In *db/db* mice (n = 4) and *LepR*^{b}*-GFP* mice (n = 4) histology was performed upon completion of physiology experiments. Mice were anesthetized with isoflurane 1%–2% and rapidly perfused

with PBS followed by ice-cold 4% paraformaldehyde in distilled water. The brains were carefully removed, postfixed in 4% paraformaldehyde for 1 h at 4°C, and cryoprotected in 20% sucrose in PBS overnight at 4°C. Then, brains were covered with O.C.T. Compound (Tissue Tek, Cat No: 4583) and frozen using 2-methylbutane on dry ice. Frozen brains were cut into 16-µm thick coronal sections on a sliding microtome and stored at –20°C until further use. Immunohistochemical staining of brain slices was performed as described previously [20, 46] with modifications. Briefly, sections were blocked for 2 h with 10% normal goat serum in PBS/0.5% TritonX-100 (PBST). The antibodies were added and incubated overnight at 4°C. The next day, sections were washed with PBST at room temperature and incubated for 2 h with secondary antibodies. The sections were washed again with PBST and cover-slipped with mounting medium for fluorescence with DAPI (4,6-diamidino-2-phenylindole, Vectashield, CA, USA).

LepR^b protein expression in the hypothalamus of *db/db* mice after infection with *Ad-LepR^b-GFP* and *LepR^b-GFP* mice was detected based on the presence of a reporter, enhanced green fluorescent protein (EGFP) [41]. Positive expression of leptin receptor in the *Ad-LepR^b*-treated *db/db* mice was confirmed by immunostaining with chicken anti-rat *LepR^b* antibody (1:100, CH14104, Neuromics, MN) and detected with goat anti-Chicken IgY secondary antibody, Alexa Fluor 568 (1:500, Cat No: A-11041).

Phenotypic identification of the LepR^b-positive cells in the hypothalamus of the *Ad-LepR^b-GFP* treated *db/db* mice and *LepR^b-GFP* mice was assessed by immunostaining for Anti-NeuN as a neuronal marker (1:100, ab104225, ABCAM, Cambridge, MA), anti-Glial Fibrillary Acidic Protein (GFAP) as an astrocyte marker, (1:100, N1506, DAKO, Carpinteria, CA), and anti-ionized calcium-binding adaptor molecule 1 (Iba1) as a microglia marker (1:100. ab178846, ABCAM, Cambridge, MA). Then, the slides were incubated with goat anti-rabbit secondary antibody, Alex Fluor 647 (1:500, Cat No: A-21245). Co-localization with MC4 was examined with rabbit polyclonal to MC4 antibodies (1:100, ab24233, ABCAM, Cambridge, MA).

Fluorescence images were examined with an Inverted Axio Observer 3 microscope (Carl Zeiss, Jena, Germany) equipped with an Axiocam 512 camera. The following filters have been used: for EGFP the led module-475 nm filter; for Alexa 647 the led module-630 nm filter, for Alexa 568 the led module-567 nm filter, and for DAPI, the led module-385 nm filter. All the images were processed and merged with the softwares Carl Zeiss Image and ImageJ (NIH). At least 300 cells per mouse were manually counted and the percentage of LepR^b-positive cells was calculated.

Statistical analysis

Data were tested for normality using Shapiro–Wilk's test. Effects of virus transfection (*Ad-LepR^b* vs *Ad-mCherry*) and treatment (leptin vs PBS), as well as their interaction (virus*treatment), on sleep studies and metabolic parameters were verified using Generalized Estimating Equations (GEE). GEE was used to obtain adjusted estimates of association between repeated measurements within subjects and also between the groups at each time point [48]. Pairwise comparisons were performed by Bonferroni's post hoc test. The effects of treatment randomization according to the crossover design were firstly tested for each dependent variable and no statistical significance was observed. The goodness of fit of each model was assessed by Quasi-likelihood under Independence Model Criterion (QIC) and the residuals were tested for normality using Q–Q plots. Statistical analyses were performed in SPSS version 20.0 (IBM SPSS Inc., Chicago, IL) and the data are represented as mean ± SEM. Statistical significance was considered at a level of $p < 0.05$.

Results

Arterial blood gas analysis

Arterial blood gas in *db/db* mice at baseline was pH 7.37 ± 0.01; $PaCO_2$ 42.3 ± 2.1 mmHg, and PaO_2 79.8 ± 6.1 mmHg. $PaCO_2$ was markedly higher and pH was lower than we previously reported in lean C57BL/6J mice (pH 7.46 ± 0.06, $PaCO_2$ 30 ± 5.0 mmHg, and PaO_2 98 ± 3.9 mmHg) [14].

Leptin receptor expression in the DMH

LepR^b and mCherry were successfully expressed in the DMH of *db/db* mice transfected with *Ad-LepR^b* (Figure 2A–C) and *Ad-mCherry* (Supplemental Figure 1). Expression of LepR^b or control mCherry was not detected in any other area of the brain. Expression of LepR^b in the DMH was confirmed both by LepR^b antibody staining (Figure 2, A and B) and by GFP fluorescence (Figure 2, C). Quantitative analysis of GFP fluorescence in *db/db* mice showed that *Ad-LepR^b* was present in 11.6% ± 1.7% of all DMH cells. LepR^b were identified in neurons by co-localizing *Ad-LepR^b-GFP* and NeuN (Figure 2, C). LepR^b was absent in astrocytes and microglia as shown by the lack of co-localization of *Ad-LepR^b-GFP* with GFAP (Figure 2, D) and IBA-1 (Figure 2, E), respectively. Nearly all *Ad-LepR^b* positive cells were MC4-positive as it was evident from co-localization of MC4 red and GFP resulting in orange color (Figure 2, F). Quantitative analysis of GFP fluorescence in DMH of *LepR^b-Cre-GFP* mice showed that LepR^b was present in a similar pattern as in *Ad-LepR^b-GFP*-transfected *db/db* mice: LepR^b was expressed in a similar percentage of cells, 9.6% ± 0.8%, and was observed exclusively in neurons (Figure 2, G), but not in astrocytes (Figure 2, H) or microglia (not shown). Co-localization of MC4 and LepR^b-GFP was detected in some cells shown with arrows. Higher magnification (Figure 2, I, insert) showed that LepR^b and MC4 co-localized in a majority of cells, but LepR^b was distributed diffusely throughout the cell, whereas MC4 was detected perinuclearly (merged blue DAPI + red MC4 resulting in purple color) suggesting that it was inactive [49]. Thus, we successfully expressed LepR^b in the DMH and the distribution of LepR^b in MC4 positive neurons resembled the natural distribution of LepR^b in *LepR^b-Cre-GFP* mice.

Basic characteristics of *db/db* mice

Characteristics of *db/db* mouse that underwent sleep recordings are shown in Table 1. Weight, age, body temperature, and food intake were not significantly different between *Ad-LepR^b* and the *Ad-mCherry* groups at the time of transfection. Body temperature increased ($p < 0.05$) and food intake decreased ($p < 0.001$) in the *Ad-LepR^b* group when treated with leptin compared to PBS.

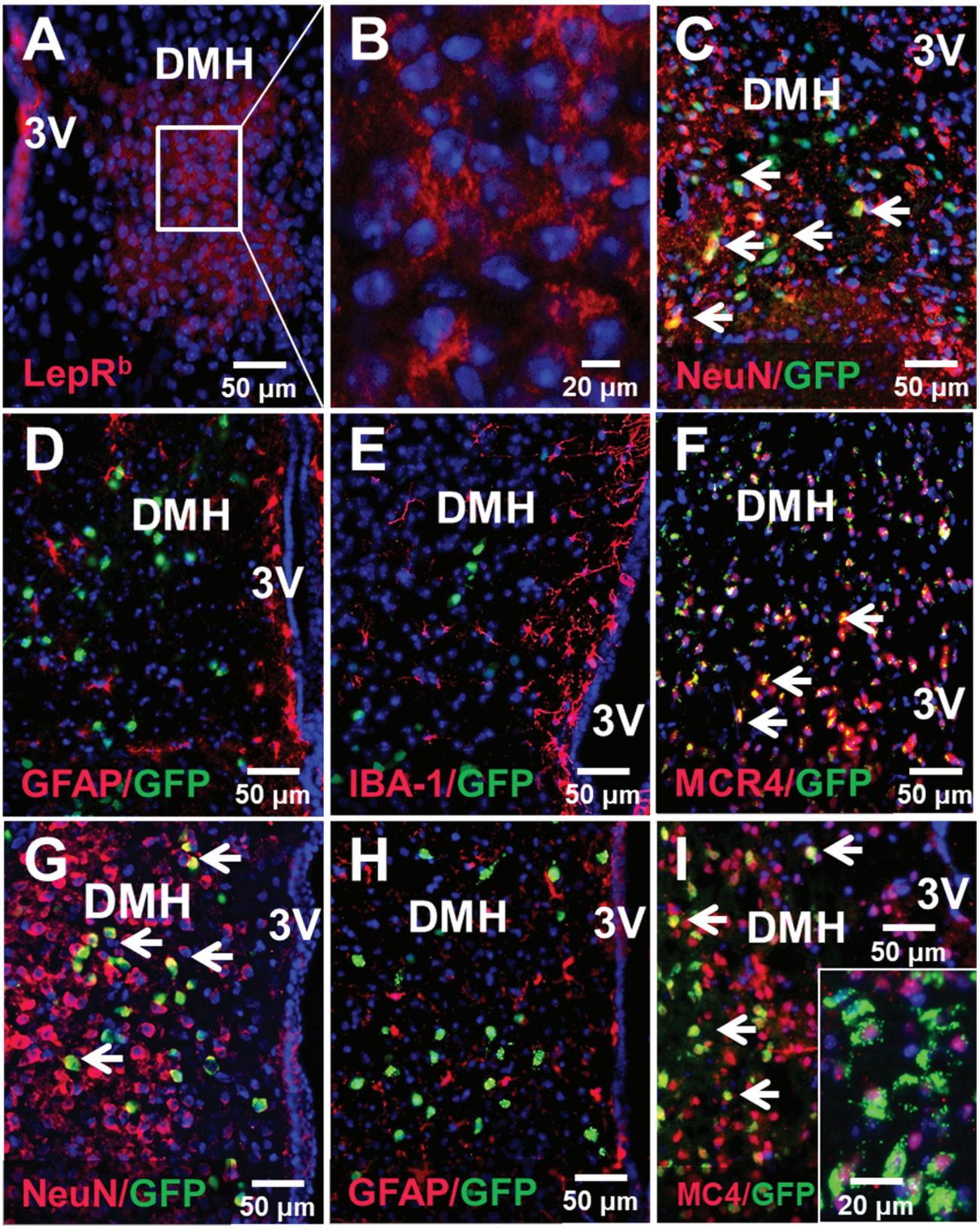

Figure 2. Localization of LepR^b in the DMH of db/db mice after *Ad-LepR*^{b} infection (A–F) compared to LepR^b in DMH of *LepR*^{b}*-Cre-GFP* mice (G–I). (A) LepR^b (in RED) was expressed in the DMH of db/db mice 9 days after *Ad-LepR*^{b} infection; DAPI (4′,6-diamidino-2-phenylindole) in BLUE. (B) Same at higher power; (C) GFP in DMH of *db/db* mice was localized in neurons (NeuN, RED) as evidenced by ORANGE color after merging (arrows), but not in (D) astrocytes (glial fibrillary acidic protein, GFAP, RED) (E) or microglia (IBA-1101, RED); (F) in *db/db* mice GFP co-localized with melanocortin 4 receptor (MC4). In *LepR*^{b}*-Cre* mice LepR^b localized in neurons (G, ORANGE), but not in astrocytes (H). (I) LepR^b co-localized with MC4 (ORANGE at lower power and co-localization at higher power, corner insert); note perinuclear location of MC4 (insert), which is typical in the inactive state [49]. 3V, third ventricle.

Table 1. Characteristics of age, weight, temperature, and food intake for *db/db* mice transfected with either *Ad-mCherry* or *Ad-LepR*^{b} and infused with PBS or leptin ICV

		Age, weeks		Weight, g		Temperature, °C		Food intake, g	
	n	Mean ± SE	Range	Mean ± SE	Range	Mean ± SE	Range	Mean ± SE	Range
Ad-mCherry									
PBS	12	15.9 ± 0.0	15.0–17.0	47.4 ± 0.9	39.4–50.6	36.1 ± 0.3	34.6–37.5	3.0 ± 0.5	2.1–5.9
Leptin	12	16.0 ± 0.1	15.0–17.1	46.9 ± 1.0	39.9–51.5	35.4 ± 0.2	34.4–36.6	3.0 ± 0.4	2.3–5.2
Ad-LepR^b									
PBS	14	15.7 ± 0.1	14.0–17.4	49.4 ± 1.3	35.7–55.4	35.8 ± 0.3	33.3–37.8	3.2 ± 0.2	1.6–4.5
Leptin	14	15.7 ± 0.1	14.0–17.0	49.8 ± 1.2	36.9–56.0	36.3 ± 0.2*	35.1–38.2	2.5 ± 0.3***	1.6–3.8

Weight was recorded prior to sleep recording. Rectal temperature was averaged between beginning and end of sleep recording. Food intake was measured for 24 h post leptin or PBS treatment. Values presented as mean values ± standard error and range.
ICV, intracerebroventricular.
*$p < 0.05$; ***$p < 0.001$.

Table 2. Sleep characteristics for *db/db* mice transfected with either *Ad-mCherry* or *Ad-LepR*^{b} and infused with PBS or leptin ICV

			Sleep time, min			Sleep Bout number, *n*		Sleep Bout length, s	
	n	Sleep efficiency, %	TST	NREM	REM	NREM	REM	NREM	REM
Ad-mCherry									
PBS	12	73.6 ± 4.3	273.0 ± 17.6	268.6 ± 17.2	4.5 ± 2.2	41.9 ± 4.9	4.7 ± 2.1	486.2 ± 96.9	44.2 ± 10.5
Leptin	12	72.3 ± 4.0	281.2 ± 20.5	274.8 ± 21.1	6.5 ± 1.4	31.4 ± 6.0	5.5 ± 1.0	446.8 ± 91.9	72.5 ± 10.4
Ad-LepR^b									
PBS	14	64.3 ± 3.7	241.0 ± 16.6	235.9 ± 16.5	5.2 ± 0.8	57.8 ± 5.3	5.0 ± 0.7	301.0 ± 50.9	65.9 ± 4.9
Leptin	14	69.6 ± 3.9	267.1 ± 19.1	266.1 ± 19.2	1.0 ± 0.3***	58.5 ± 8.3	1.3 ± 0.4***	447.6 ± 115.6	34.2 ± 9.6

Values presented as mean values ± standard error.
ICV, intracerebroventricular; TST, total sleep time.
***$p < 0.001$.

Effect of leptin signaling in DMH on sleep architecture

Sleep architecture for all groups is described in Table 2. There was no significant difference in sleep efficiency, total sleep time, NREM sleep time, NREM sleep bout number or bout length between *Ad-LepR*^{b}, and *Ad-mCherry* groups at baseline, nor was there an effect of ICV leptin. Leptin induced a 4–6-fold decrease in REM sleep time in *Ad-LepR*^{b} transfected mice compared to PBS infusion ($p < 0.001$) and compared to *Ad-mCherry* transfected mice treated with leptin ($p < 0.001$). In fact, leptin abolished REM sleep entirely in 6 out of 14 *Ad-LepR*^{b}-infected mice, and, in the remaining mice, it was only 1 min long, 0.4% of total sleep time (Table 2). There was no significant difference in REM sleep bout length between any of the groups, but REM sleep bout number was significantly lower after leptin treatment in mice transfected with *Ad-LepR*^{b} ($p < 0.001$).

Representative polysomnography recordings of NREM sleep in *db/db* mice transfected with either *Ad-LepR*^{b} or *Ad-mCherry* during PBS and leptin treatments are shown in Figure 3. Leptin treatment did not change the respiratory pattern in *Ad-mCherry* transfected mice (Figure 3, Left Panels). In contrast, ventilation visually increased after leptin administration in the *Ad-LepR*^{b} transfected mice (Figure 3, Right Panels). The respiratory pattern in REM sleep was not affected by types of virus or injection (Supplemental Figure 2).

Effect of leptin on non-flow limited breathing during sleep

In mice transfected with *Ad-LepR*^{b}, administration of leptin to the lateral ventricle increased minute ventilation (nV_E) during NREM sleep from 0.78 ± 0.06 to 0.97 ± 0.07 mL/min/g, $p < 0.01$, whereas no effect was observed in mice transfected with *Ad-mCherry* (0.72 ± 0.06 mL/min/g with PBS and 0.70 ± 0.07 mL/min/g with leptin) (Figure 4, A). This 24% increase in minute ventilation was attributed to an increase in tidal volume (V_T) from 0.19 ± 0.01 mL to 0.22 ± 0.02 mL ($p < 0.001$), whereas respiratory rate (RR) was unchanged (Figure 4, B and C).

In *Ad-LepR*^{b}-transfected mice, ICV leptin increased maximal inspiratory flow ($V_I$max) during non-flow limited breathing by 20%, from 3.40 ± 0.25 mL/s to 4.09 ± 0.28 mL/s (Figure 5, A) and increased mean inspiratory flow rate (MIFR) by 24%, from 1.91 ± 0.14 mL/s to 2.37 ± 0.15 mL/s (Figure 5, B). Leptin had no significant effect in mice transfected with *Ad-mCherry*.

During REM sleep in *Ad-mCherry* transfected mice treated with PBS, nV_E was 0.68 ± 0.11 mL/min/g, $V_I$max was 2.1 ± 0.21 mL/s, and MIFR was 1.28 ± 0.15 mL/s. There were no significant effects of *Ad-LepR*^{b} or leptin. However, there was large variability between the animals due to very short REM sleep duration, especially in the *Ad-LepR*^{b} group after leptin treatment (Table 2).

Effect of leptin on upper airway obstruction in DMH-Ad-LepR^b transfected *db/db* mice

The percentage of inspiratory flow limited breaths was negligible for all time points during NREM sleep in both the *Ad-mCherry* and the *Ad-LepR*^{b} groups. *db/db* mice developed upper airway obstruction exclusively during REM sleep (Supplemental Figure 2). The prevalence of inspiratory flow limited breaths in REM sleep after PBS treatment was the

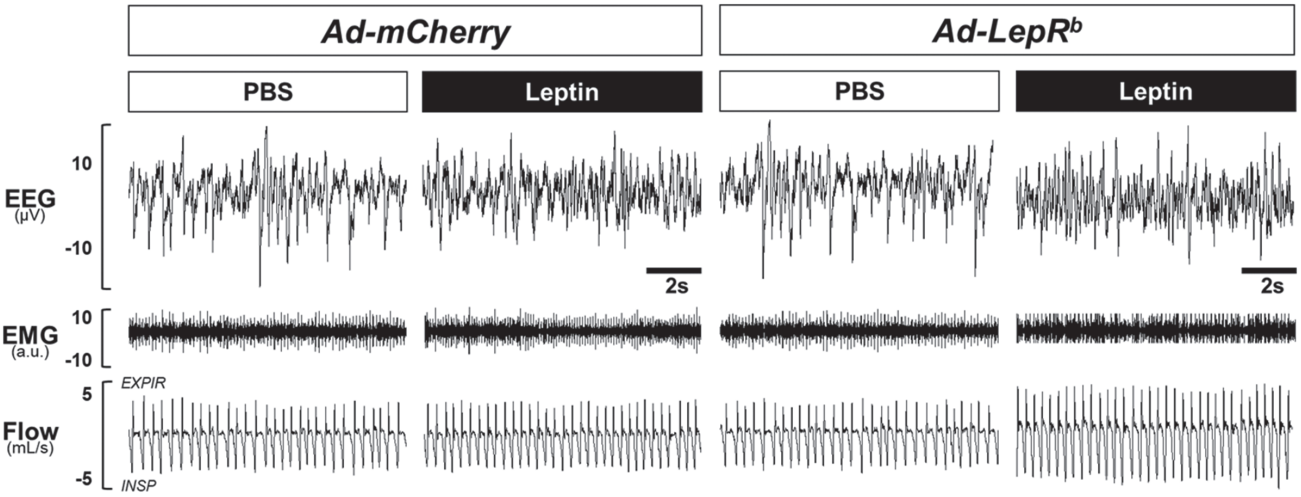

Figure 3. Representative NREM sleep recordings in *db/db* mice transfected with (A) *Ad-mCherry* or (B) *Ad-LepR*^{b} in the dorsomedial hypothalamus. Intracerebroventricular administration of leptin augmented ventilation in *Ad-LepR*^{b} mice without altering sleep architecture. No leptin effect was observed after *Ad-mCherry* transfection.

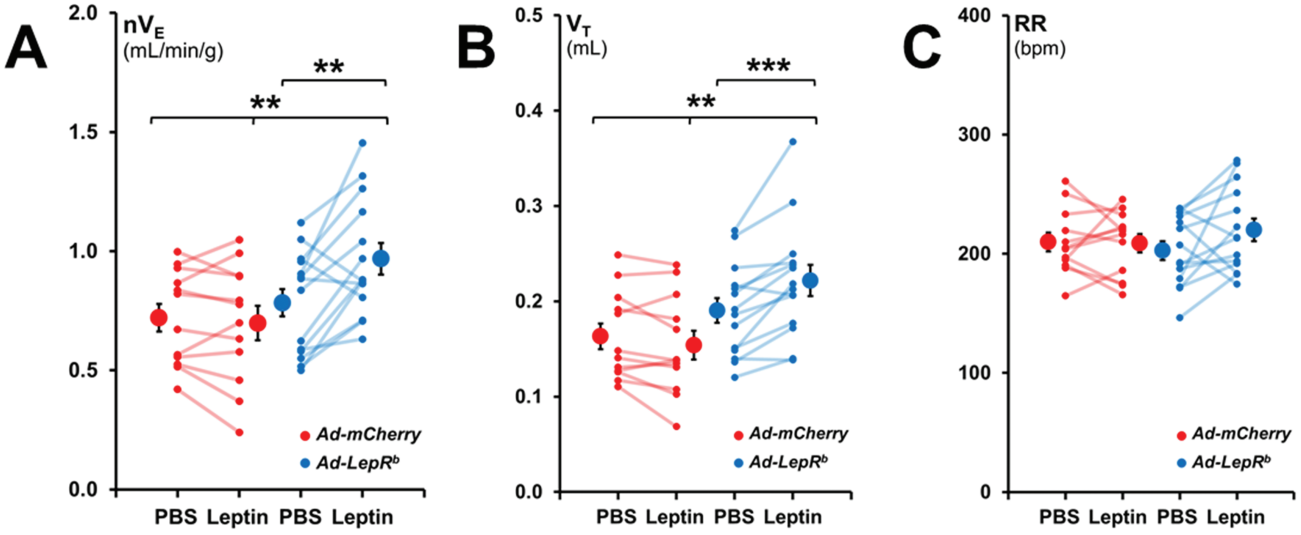

Figure 4. Normalized minute ventilation (nV_E), tidal volume (V_T), and respiratory rate (RR) in non-flow limited breathing during NREM sleep. Each line represents individual mice; mean values ± standard errors are shown. Leptin infusion augmented nV_E in the *Ad-LepR*^{b} group compared to PBS injection and the *Ad-mCherry* group. Changes in nV_E were caused by an increase in V_T. $^{**}p < 0.01$; $^{***}p < 0.001$.

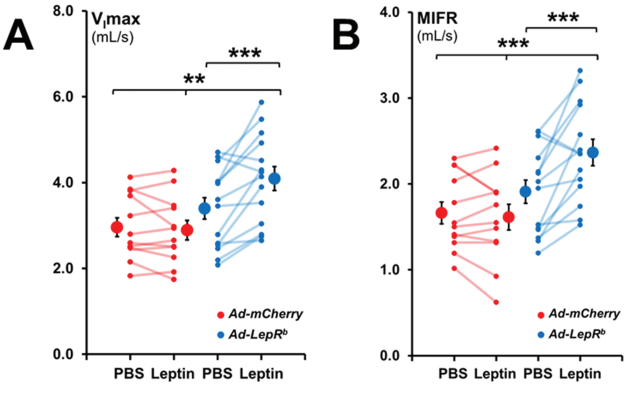

Figure 5. Maximum inspiratory flow ($V_I$max) and mean inspiratory flow rate (MIFR) in NREM sleep during non-flow limited breathing. Each line represents individual mice; mean values ± standard errors are shown. Leptin infusion increased $V_I$max and MIFR in NREM in *Ad-LepR*^{b} mice compared to PBS injection and the *Ad-mCherry* group. $^{**}p < 0.01$; $^{***}p < 0.001$.

same in the *Ad-mCherry* and the *Ad-LepR*^{b} groups. Leptin had no effect on the percentage of inspiratory flow limited breaths in REM sleep in the *Ad-LepR*^{b}-treated mice, 14.9% ± 3.4% of all breaths after PBS and 7.8% ± 2.1% after leptin. Flow limited breathing in REM sleep in PBS infused *Ad-mCherry* mice was characterized by nV_E of 0.49 ± 0.05 mL/min/g, $V_I$max of 1.41 ± 0.18 mL/s, and MIFR of 0.95 ± 0.12 mL/s. There was no effect of treatment, but similarly to non-obstructive breathing, large variability between animals was observed due to very short REM duration, particularly in the *Ad-LepR*^{b} group after leptin (Table 2).

Leptin had no effect on metabolism in DMH Ad-LepR^b transfected *db/db* mice

In order to examine, if the increase in minute ventilation was due to an increase in CO_2 production by leptin, we monitored the mice in metabolic cages (Figure 6). In mice transfected with

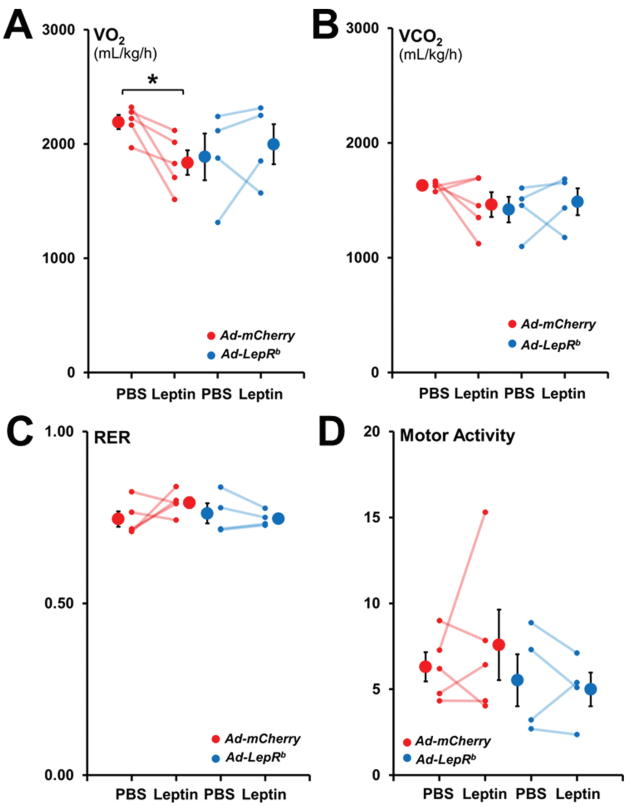

Figure 6. Energy expenditure and motor activity during the light phase in *db/db* mice infected with *Ad-LepR*^{b}-GFP or *Ad-mCherry*. Each line represents individual mice; mean values ± standard errors are shown. There were no changes in (A) total oxygen consumption (VO_2), (B) total carbon dioxide production (VCO_2), (C) respiratory exchange ratio (RER) and (D) total motor activity between the *Ad-LepR*^{b} and *Ad-mCherry* groups with either PBS or leptin infusions. $^*p < 0.05$.

Ad-LepR^b in the DMH, ICV leptin did not affect energy expenditure or motor activity. Similar data were obtained in mice transfected with *Ad-mCherry*, except for a curious and inexplicable decrease in VO_2 with leptin administration.

Discussion

The main finding of our study is that targeted expression of LepR^b in the DMH in an animal model with SDB (LepR^b-deficient *db/db* mice) resulted in a beneficial sustained increase in minute ventilation during NREM sleep in response to ICV leptin infusion. We also report several other novel findings. *First*, LepR^b-deficient obese *db/db* mice exhibit chronic alveolar hypoventilation, which is similar to humans with OHS. *Second*, adenoviral vector-driven DMH transfection of *LepR*^{b} resulted in LepR^b expression exclusively in neurons, and these neurons were MC4 positive in a pattern similar to *LepR*^{b}*-Cre-GFP* mice. *Third*, leptin-induced hyperventilation mediated by LepR^b (+) DMH neurons was not associated with an increase in VCO_2 implicating stimulation of respiratory control centers. *Fourth*, ICV leptin suppressed REM sleep acting upon LepR^b (+) DMH neurons. *Fifth*, *db/db* mice exhibited upper airway obstruction during REM sleep, which was not affected by expression of LepR^b in DMH.

db/db mice exhibit alveolar hypoventilation

Compared to our historic data in lean and diet-induced obese C57BL/6J mice [14], *db/db* mice had excellent sleep efficiency and had less fragmented NREM sleep in the barometric plethysmography chamber. Total REM sleep time at baseline was similar to diet-obese mice and decreased compared to lean mice [14] due to a decreased number of REM sleep bouts. Our data provided first demonstration that leptin-resistant obese *db/db* mice hypoventilate chronically, similar to leptin deficient *ob/ob* mice [27] and leptin-resistant diet-induced obese mice [14]. Awake unrestrained unanesthetized *db/db* mice had compensated respiratory acidosis with $PaCO_2$ of 42 mmHg, which was similar to that in *ob/ob* mice [27] and slightly higher than $PaCO_2$ of 39 mmHg previously reported in diet-induced obese mice [14]. In contrast, lean mice on the same genetic background had $PaCO_2$ of 30–33 mmHg [14, 27]. Sleep studies in *db/db* mice demonstrated hypoventilation during NREM sleep with average nV_E of 0.78 mL/min/g, compared to our historic data of 1.2–1.3 mL/min/g in lean mice [14], as a cause of CO_2 retention. *ob/ob* and diet-induced obese mice showed the same levels of hypoventilation as *db/db* mice [14, 18, 19]. However, *ob/ob* and *db/db* mice breathe at lower V_T and higher RR than diet-induced obese mice (~0.19 vs 0.23 mL and >200 vs 150 breaths per minute, respectively), which could lead to higher dead space ventilation and lower alveolar ventilation resulting in higher CO_2 levels observed in our studies [14, 18, 19, 27]. Thus, leptin-resistant *db/db* and diet-induced obese mice as well as leptin-deficient *ob/ob* mice exhibit obesity hypoventilation, similar to obese humans with OHS [8, 50]. OHS leads to high mortality with 23% untreated patients dying during the 18-month observation period [8, 51]. Understanding of mechanisms by which leptin acts on respiratory centers in the brain to increase ventilation is important for future therapy of SDB.

The effect of leptin on control of breathing and the role of LepR^b signaling in DMH MC4 (+) neurons

Leptin-LepR^b signaling in the DMH increases metabolic rate by activating thermogenesis in brown adipose tissue [52, 53]. In our study, administration of leptin ICV to LepR^b-deficient *db/db* mice expressing LepR^b receptor exclusively in DMH induced a modest increase in core body temperature of 0.5°C (Table 1), but there was no significant changes in VCO_2 or VO_2 (Figure 6). The lack of metabolic response could be attributed to relatively low levels of LepR^b, which was detected only in 11.6% of DMH cells, in the absence of LepR^b receptor expression in other hypothalamic [54] and medullary nuclei [55] involved in regulation of metabolism. Nevertheless, even this low level of LepR^b expression restored sensitivity to respiratory effects of leptin. ICV leptin increased minute ventilation in NREM sleep without concurrent increases in VCO_2 or physical activity, which suggests stimulation of respiratory control centers in the brain. In fact, the magnitude of the effect of leptin signaling in DMH on minute ventilation in our current study was identical to increases induced by leptin *via* signaling in the entire brain of *ob/ob* mice and diet-induced obese mice in our previous studies [19, 20, 56].

Bassi *et al.* microinjected leptin into the ventrolateral medulla of *ob/ob* mice, specifically into the retrotrapezoid nucleus/parafacial respiratory group [57], a primary site for central chemoreception [58–60], and found an increase in the hypercapnic ventilatory

response in awake animals. Microinjection of leptin into the nucleus of the solitary tract (NTS) significantly increased respiratory activity in anesthetized rats under hypercapnic conditions [61], and optogenetic stimulation of LepR^b (+) NTS neurons in mice mimicked the respiratory stimulation after systemic leptin administration [55]. LepR^b (+) DMH neurons may stimulate breathing *via* their projections to these medullary nuclei, but overall mechanisms of respiratory effects of leptin in DMH remain unknown.

Another intriguing finding of our study was that *Ad-LepR^b* transfection resulted in LepR^b expression in MC4 (+) neurons of DMH (Figure 2). Furthermore, MC4 staining of DMH in *LepR^b-Cre*-GFP mice showed a similar pattern. MC4 activity is regulated by leptin [62, 63]. MC4 signaling increases metabolic rate by inducing metabolic uncoupling in brown adipose tissue [64]. The melanocortin system is also involved in respiratory effects of leptin. Mice producing agouti-related peptide with deficient leptin and melanocortin signaling have suppressed hypercapnic ventilatory response [65]. An MC4 blocker SHU abolished leptin-induced respiratory chemosensitivity [66]. Thus, MC4 signaling may play a role in mediating respiratory effects of leptin signaling in DMH.

The effect of leptin on upper airway patency during sleep

Our data also showed that *db/db* mice exhibit mild inspiratory flow limitation at baseline, exclusively in REM sleep. We have previously reported very low prevalence of obstructed breaths in NREM sleep in *ob/ob* mice (<1%–3%), whereas prevalence of obstructed breaths in REM sleep was higher [18, 19]. More severe impairment of upper airway patency could be related to older age or higher body weight of *ob/ob* mice in the previous studies, 65–70 g [18, 19] compared to 47–50 g in *db/db* mice in the current study (Table 1). In contrast, diet-induced obese mice showed much higher prevalence of obstructed breathing in both NREM and REM sleep, 13%–15% and 35%–45% respectively, despite having similar weight to *db/db* mice [14, 20]. Thus, diet-induced obesity appears to predispose to OSA compared to genetic models of leptin deficiency and resistance.

Our previous work demonstrated that leptin acts in the brain to relieve upper airway obstruction during sleep, both in leptin-deficient *ob/ob* mice [19] and in leptin-resistant diet-induced obese animals [20]. LepR^b was not detected in the hypoglossal motoneurons, but there was evidence that LepR^b positive neurons are synaptically connected to hypoglossal neurons [20]. Moreover, leptin activated hypoglossal motoneurons in brain slices [56]. Indirect evidence indicated that leptin acts in the forebrain, possibly in DMH, to regulate upper airway patency during sleep [19]. Our current study did not confirm this report showing that leptin had no effect on flow limited breathing in *db/db* mice expressing LepR^b in DMH neurons. However, leptin substantially shortened REM sleep, from 5.2 to 1 min and the prevalence of upper airway obstruction at control conditions was only 14.9%. Thus, our data on the role of leptin signaling in DMH in the pathogenesis of OSA are inconclusive.

Leptin and sleep

We have previously reported that ICV leptin shortened REM sleep in *ob/ob* mice [19], which was consistent with previous data in rats [67]. In humans, a sharp decline in leptin levels through the night was associated with REM sleep rebound [68]. Taken together, this data suggests that leptin shortens REM sleep, possibly *via* LepR^b signaling in the DMH. The role of DMH in REM sleep regulation is insufficiently studied. Several hypothalamic mediators, including melanin concentrating hormone [69] and hypocretin [70–72], may impact REM sleep, but neurons producing these molecules were located predominantly to the lateral hypothalamus. Chen *et al.* showed that galanin-expressing GABAergic neurons in the DMH constitute two different neuronal populations with opposing effects on REM sleep [73], but the relevance of this finding for our study is uncertain. Finally, LepR^b signaling in DMH may decrease REM sleep indirectly by increasing body temperature [74], but the effect of leptin on body temperature in our study was modest.

Limitations of the study

Our study had a number of limitations. *First*, mice were heavily instrumented and sleep was recorded only for 6 h after ICV injections, which could affect the quality of sleep. In order to account for these inevitable confounders we compared PBS with leptin within the same mice and *Ad-LepR^b* with control virus. *Second*, an adenoviral vector may induce non-specific adverse effects in mice. In order to counter this problem we used control *Ad-Cherry* vector and completed all studies within 13–20 days after transfection. Furthermore, we found that *Ad-LepR^b* by itself did not induce any metabolic or respiratory effects prior to leptin injections. *Third, db/db* mice have very high plasma leptin levels at baseline [14], nevertheless ICV delivery of supplemental leptin was required to induce respiratory effects. This phenomenon may be attributable to the impaired blood–brain barrier permeability for leptin [75] and/or the lack of LepR^b signaling in other brain nuclei implicated in respiratory control. *Fourth,* leptin significantly decreased REM sleep in *Ad-LepR^b* transfected mice and, therefore, respiratory analysis during very short stretches of REM sleep was inconclusive. *Fifth*, although our model allowed us to identify effects of leptin on control of breathing, *db/db* mice appeared to be a suboptimal model to study effects of leptin on upper airway during sleep, because upper airway obstruction was present only during short episodes of REM sleep. Given that mice with diet-induced obesity showed more severe inspiratory flow limitation during both NREM and REM sleep [14, 20] than *ob/ob* [18, 19] and *db/db* mice, chemogenetic and/or optogenetic approaches in LepR^b-Cre diet-induced obese mice may be more promising for OSA research. *Sixth,* the goal of our study was to establish if LepR^b DMH neurons are involved in control of breathing, but we did not examine synaptic projections of these neurons to downstream respiratory control centers in the brainstem.

In conclusion, leptin stimulates ventilation by acting on LepR^b (+) neurons in DMH and this effect is independent of metabolism. Further elucidation of molecular make up of LepR^b (+) DMH neurons and their projections to respiratory control centers, including *in vivo* and *in vitro* physiology experiments targeting these neurons, may lead to new therapies for OHS, a common and lethal condition, and novel treatment strategies for other forms of hypoventilation characterized by diminished CNS output.

Supplementary material

Supplementary material is available at *SLEEP* online.

Funding

This study was supported by the grants from the National Institutes of Health R01 HL128970, R01 HL133100, R01 HL13892, and R61 HL156240 (all to VYP), and American Heart Association Career Development Awards 19CDA34700025 (MKS) and 19CDA34660245 (TFC).

Disclosure Statements

All authors report no support from commercial entities or other financial or non-financial conflicts of interest.

Data Availability

This manuscript preprint 10.1101/2020.09.29.318758 has posted on the repository bioRxiv and is found at https://biorxiv.org/cgi/content/short/2020.09.29.318758v1.

References

1. Flegal KM, *et al*. Prevalence and trends in obesity among US adults, 1999-2008. *JAMA*. 2010;**303**(3):235–241.
2. Young T, *et al*. The occurrence of sleep-disordered breathing among middle-aged adults. *N Engl J Med*. 1993;**328**(17):1230–1235.
3. Vgontzas AN, *et al*. Sleep apnea and daytime sleepiness and fatigue: relation to visceral obesity, insulin resistance, and hypercytokinemia [see comments]. *J ClinEndocrinolMetab*. 2000;**85**(0021-972X):1151–1158.
4. Tufik S, *et al*. Obstructive sleep apnea syndrome in the Sao Paulo Epidemiologic Sleep Study. *Sleep Med*. 2010;**11**(5):441–446.
5. Punjabi NM, *et al*. The association between daytime sleepiness and sleep-disordered breathing in NREM and REM sleep. *Sleep*. 2002;**25**(3):307–314.
6. Remmers JE, *et al*. Pathogenesis of upper airway occlusion during sleep. *J Appl Physiol Respir Environ Exerc Physiol*. 1978;**44**(6):931–938.
7. Gastaut H, *et al*. Polygraphic study of diurnal and nocturnal (hypnic and respiratory) episodal manifestations of Pickwick syndrome. *RevNeurol(Paris)*. 1965;**112**(6):568–579.
8. Mokhlesi B. Obesity hypoventilation syndrome: a state-of-the-art review. *Respir Care*. 2010;**55**(10):1347–62; discussion 1363.
9. Sullivan CE, *et al*. Reversal of obstructive sleep apnoea by continuous positive airway pressure applied through the nares. *Lancet*. 1981;**1**(8225):862–865.
10. Abbey NC, *et al*. Benefit of nasal CPAP in obstructive sleep apnea is due to positive pharyngeal pressure. *Sleep*. 1989;**12**(5):420–422.
11. Howard ME, *et al*. A randomised controlled trial of CPAP versus non-invasive ventilation for initial treatment of obesity hypoventilation syndrome. *Thorax*. 2017;**72**(5):437–444.
12. Kribbs NB, *et al*. Objective measurement of patterns of nasal CPAP use by patients with obstructive sleep apnea. *Am Rev Respir Dis*. 1993;**147**(4):887–895.
13. Hernandez AB, *et al*. Novel whole body plethysmography system for the continuous characterization of sleep and breathing in a mouse. *J Appl Physiol (1985)*. 2012;**112**(4):671–680.
14. Fleury Curado T, *et al*. Sleep-disordered breathing in C57BL/6J mice with diet-induced obesity. *Sleep*. 2018;**41**(8). doi: 10.1093/sleep/zsy089
15. Condos R, *et al*. Flow limitation as a noninvasive assessment of residual upper-airway resistance during continuous positive airway pressure therapy of obstructive sleep apnea. *Am J Respir Crit Care Med*. 1994;**150**(2):475–480.
16. Schwartz AR, *et al*. Mechanism of inspiratory flow limitation in the isolated canine upper airway during neuromuscular blockade. *Am Rev Respir Dis*. 1989;**139**:A79.
17. Polotsky M, *et al*. Effects of leptin and obesity on the upper airway function. *J Appl Physiol (1985)*. 2012;**112**(10):1637–1643.
18. Pho H, *et al*. The effect of leptin replacement on sleep-disordered breathing in the leptin-deficient ob/ob mouse. *J Appl Physiol (1985)*. 2016;**120**(1):78–86.
19. Yao Q, *et al*. Localizing effects of leptin on upper airway and respiratory control during Sleep. *Sleep*. 2016;**39**(5):1097–1106.
20. Berger S, *et al*. Intranasal leptin relieves sleep-disordered breathing in mice with diet-induced obesity. *Am J Respir Crit Care Med*. 2019;**199**(6):773–783.
21. Schwartz AR, *et al*. Obesity and obstructive sleep apnea: pathogenic mechanisms and therapeutic approaches. *Proc Am Thorac Soc*. 2008;**5**(2):185–192.
22. Polotsky M, *et al*. Effect of age and weight on upper airway function in a mouse model. *J Appl Physiol (1985)*. 2011;**111**(3):696–703.
23. Shapiro SD, *et al*. Leptin and the control of pharyngeal patency during sleep in severe obesity. *J Appl Physiol (1985)*. 2014;**116**(10):1334–1341.
24. Friedman JM. Leptin at 14 y of age: an ongoing story. *Am J Clin Nutr*. 2009;**89**(3):973S–979S.
25. Halaas JL, *et al*. Weight-reducing effects of the plasma protein encoded by the obese gene. *Science*. 1995;**269**(5223):543–546.
26. Spiegelman BM, *et al*. Obesity and the regulation of energy balance. *Cell*. 2001;**104**(4):531–543.
27. O'donnell CP, *et al*. Leptin prevents respiratory depression in obesity. *Am J Respir Crit Care Med*. 1999;**159**(5 Pt 1):1477–1484.
28. Phipps PR, *et al*. Association of serum leptin with hypoventilation in human obesity. *Thorax*. 2002;**57**(1):75–76.
29. Considine RV, *et al*. Serum immunoreactive-leptin concentrations in normal-weight and obese humans. *N Engl J Med*. 1996;**334**(5):292–295.
30. Maffei M, *et al*. Leptin levels in human and rodent: measurement of plasma leptin and ob RNA in obese and weight-reduced subjects. *Nat Med*. 1995;**1**(11):1155–1161.
31. Ip MSM, *et al*. Serum leptin and vascular risk factors in obstructive sleep apnea. *Chest*. 2000;**118**(3):580–586.
32. Berger S, *et al*. Leptin and leptin resistance in the pathogenesis of obstructive sleep apnea: a possible link to oxidative stress and cardiovascular complications. *Oxid Med Cell Longev*. 2018;**2018**:5137947.
33. Yee BJ, *et al*. Treatment of obesity hypoventilation syndrome and serum leptin. *Respiration*. 2006;**73**(2):209–212.
34. Schwartz MW, *et al*. Cerebrospinal fluid leptin levels: relationship to plasma levels and to adiposity in humans. *Nat Med*. 1996;**2**(5):589–593.
35. Banks WA, *et al*. Impaired transport of leptin across the blood-brain barrier in obesity. *Peptides*. 1999;**20**(11):1341–1345.
36. Bassi M, *et al*. Central leptin replacement enhances chemorespiratory responses in leptin-deficient mice

independent of changes in body weight. *Pflugers Arch*. 2012;**464**(2):145–153.
37. Scarpace PJ, *et al*. Leptin resistance: a prediposing factor for diet-induced obesity. *Am J Physiol Regul Integr Comp Physiol*. 2009;**296**(3):R493–R500.
38. Wauman J, *et al*. Leptin receptor signaling: pathways to leptin resistance. *Front Biosci (Landmark Ed)*. 2011;**16**:2771–2793.
39. Tartaglia LA, *et al*. Identification and expression cloning of a leptin receptor, OB-R. *Cell*. 1995;**83**(7):1263–1271.
40. Friedman J. The long road to leptin. *J Clin Invest*. 2016;**126**(12):4727–4734.
41. Scott MM, *et al*. Leptin targets in the mouse brain. *J Comp Neurol*. 2009;**514**(5):518–532.
42. Kishi T, *et al*. Expression of melanocortin 4 receptor mRNA in the central nervous system of the rat. *J Comp Neurol*. 2003;**457**(3):213–235.
43. Clément K, *et al*. MC4R agonism promotes durable weight loss in patients with leptin receptor deficiency. *Nat Med*. 2018;**24**(5):551–555.
44. Kühnen P, *et al*. Proopiomelanocortin deficiency treated with a melanocortin-4 receptor agonist. *N Engl J Med*. 2016;**375**(3):240–246.
45. Pillai S, *et al*. Severe obstructive sleep apnea in a child with melanocortin-4 receptor deficiency. *J Clin Sleep Med*. 2014;**10**(1):99–101.
46. Caballero-Eraso C, *et al*. Leptin acts in the carotid bodies to increase minute ventilation during wakefulness and sleep and augment the hypoxic ventilatory response. *J Physiol*. 2019;**597**(1):151–172.
47. Drorbaugh JE, *et al*. A barometric method for measuring ventilation in newborn infants. *Pediatrics*. 1955;**16**(1):81–87.
48. Zeger SL, *et al*. Longitudinal data analysis for discrete and continuous outcomes. *Biometrics*. 1986;**42**(1):121–130.
49. McDaniel FK, *et al*. Constitutive cholesterol-dependent endocytosis of melanocortin-4 receptor (MC4R) is essential to maintain receptor responsiveness to α-melanocyte-stimulating hormone (α-MSH). *J Biol Chem*. 2012;**287**(26):21873–21890.
50. Bickelmann AG, *et al*. Exteme obesity associated with alveolar hypoventilation-a pickwickian syndrome. *Am J Med*. 1956;**21**:811–818.
51. Budweiser S, *et al*. Mortality and prognostic factors in patients with obesity-hypoventilation syndrome undergoing noninvasive ventilation. *J Intern Med*. 2007;**261**(4):375–383.
52. Rezai-Zadeh K, *et al*. Leptin receptor neurons in the dorsomedial hypothalamus are key regulators of energy expenditure and body weight, but not food intake. *Mol Metab*. 2014;**3**(7):681–693.
53. Enriori PJ, *et al*. Leptin action in the dorsomedial hypothalamus increases sympathetic tone to brown adipose tissue in spite of systemic leptin resistance. *J Neurosci*. 2011;**31**(34):12189–12197.
54. Yu S, *et al*. Preoptic leptin signaling modulates energy balance independent of body temperature regulation. *Elife*. 2018;**7**:e33505.
55. Do J, *et al*. A leptin-mediated neural mechanism linking breathing to metabolism. *Cell Rep*. 2020;**33**(6):108358.
56. Freire C, *et al*. Intranasal leptin prevents opioid-induced sleep-disordered breathing in obese mice. *Am J Respir Cell Mol Biol*. 2020;**63**(4):502–509.
57. Bassi M, *et al*. Leptin into the ventrolateral medulla facilitates chemorespiratory response in leptin-deficient (ob/ob) mice. *Acta Physiol (Oxf)*. 2014;**211**(1):240–248.
58. Guyenet PG, *et al*. Central CO2 chemoreception and integrated neural mechanisms of cardiovascular and respiratory control. *J Appl Physiol (1985)*. 2010;**108**(4):995–1002.
59. Guyenet PG, *et al*. Neural control of breathing and CO2 homeostasis. *Neuron*. 2015;**87**(5):946–961.
60. Guyenet PG, *et al*. Interdependent feedback regulation of breathing by the carotid bodies and the retrotrapezoid nucleus. *J Physiol*. 2018;**596**(15):3029–3042.
61. Inyushkina EM, *et al*. Mechanisms of the respiratory activity of leptin at the level of the solitary tract nucleus. *Neurosci Behav Physiol*. 2010;**40**(7):707–713.
62. Schwartz MW, *et al*. Leptin increases hypothalamic pro-opiomelanocortin mRNA expression in the rostral arcuate nucleus. *Diabetes*. 1997;**46**(12):2119–2123.
63. Yaswen L, *et al*. Obesity in the mouse model of pro-opiomelanocortin deficiency responds to peripheral melanocortin. *Nat Med*. 1999;**5**(9):1066–1070.
64. Scarpace PJ, *et al*. Leptin increases uncoupling protein expression and energy expenditure. *Am J Physiol*. 1997;**273**(1 Pt 1):E226–E230.
65. Polotsky VY, *et al*. Impact of interrupted leptin pathways on ventilatory control. *J Appl Physiol (1985)*. 2004;**96**(3):991–998.
66. Bassi M, *et al*. Activation of the brain melanocortin system is required for leptin-induced modulation of chemorespiratory function. *Acta Physiol (Oxf)*. 2015;**213**(4):893–901.
67. Sinton CM, *et al*. The effects of leptin on REM sleep and slow wave delta in rats are reversed by food deprivation. *J Sleep Res*. 1999;**8**(3):197–203.
68. Olson CA, *et al*. Percentage of REM sleep is associated with overnight change in leptin. *J Sleep Res*. 2016;**25**(4):419–425.
69. Vetrivelan R, *et al*. Melanin-concentrating hormone neurons specifically promote rapid eye movement sleep in mice. *Neuroscience*. 2016;**336**:102–113.
70. Galas L, *et al*. Immunohistochemical localization and biochemical characterization of hypocretin/orexin-related peptides in the central nervous system of the frog Rana ridibunda. *J Comp Neurol*. 2001;**429**(2):242–252.
71. Hara J, *et al*. Genetic ablation of orexin neurons in mice results in narcolepsy, hypophagia, and obesity. *Neuron*. 2001;**30**(2):345–354.
72. Goforth PB, *et al*. Leptin acts via lateral hypothalamic area neurotensin neurons to inhibit orexin neurons by multiple GABA-independent mechanisms. *J Neurosci*. 2014;**34**(34):11405–11415.
73. Chen KS, *et al*. A hypothalamic switch for REM and non-REM sleep. *Neuron*. 2018;**97**(5):1168–1176.e4.
74. Harding EC, *et al*. The temperature dependence of sleep. *Front Neurosci*. 2019;**13**:336.
75. Balland E, *et al*. Hypothalamic tanycytes are an ERK-gated conduit for leptin into the brain. *Cell Metab*. 2014;**19**(2):293–301.